Paper: ASAT-14-046-SP

14th International Conference on
AEROSPACE SCIENCES & AVIATION TECHNOLOGY,
ASAT - 14 – May 24 - 26, 2011, Email: asat@mtc.edu.eg
Military Technical College, Kobry Elkobbah, Cairo, Egypt
Tel: +(202) 24025292 –24036138, Fax: +(202) 22621908

Hybrid Approach to Passive Ranging with Two Infrared Non-Imaging Sensors

Srdan T. Mitrovic*, Goran D. Dikic* and Zeljko M. Durovic†

Abstract: In this paper the principle of triangulation is used as a basic method for range estimation. However, when the target directions are nearly collinear relative to the baseline the ratio of IR energy absorbed at the end of a baseline has to be introduced in a measurement vector to obtain acceptable results. In that case, a recursive estimator for the extinction coefficient that describes the influence of the atmosphere also must be applied. Both methods are implemented within the extended Kalman filter type target state estimator. The results obtained by simulations and experimental data processing show the advantages but also the disadvantages caused by saturation effect when the target is close enough to one of the sensors. The appropriate hybrid approach in application of algorithms, triangulation and proposed method with extended measurement vector, is suggested as a solution.

Keywords: Extended Kalman filter, target tracking, fuzzy logic, hybrid approach.

Introduction

Target tracking and detection based on active sensors often is impossible on modern battlefield. Sensors can be quickly detected and destroyed by homing missiles. The use of passive infrared (IR) sensors is suggested as a solution [1]. They are recognized as providing a precise bearing only target location. Range information can also be extracted through fusion of data from two or more such sensors. An overview of the existing literature devoted to these topics suggests two main approaches. One of them is to design efficient data fusion obtained from the sensor net-work [2, 3], while the other addresses the synthesis of intelligent algorithms for non-measurable distance estimation based on measurable angles [4]. In a case where only two passive sensors are used (the so-called single baseline method), there is a direction in which all precision in the triangulated target range is lost. This phenomenon is known as 'geometric dilution of precision' (GDOP). A solution based on use of two orthogonal baselines is offered in [5]. The individual performance of each of the baselines follows the mathematics of the single baseline model. Thus, it is possible to eliminate the geometric dilution problem by switching between baselines at performance crossing points. It can be shown that the crossover points depend primarily on the ratio of the two baseline lengths [5]. Additionally, in the early 1960s, several patents were approved which related a 'hot' target's IR signal attenuation to range [6, 7]. Both of these schemes applied the principle that the ratio of signal attenuation in two narrow IR bands, with known but nominally different atmospheric attenuation coefficients, could be related to range.

* Military Academy, Generala Pavla Jurisica Sturma 33, 11000 Belgrade, Serbia, / srdjan.mitrovic@va.mod.gov.rs / grandi@beotel.net

† School of Electrical Engineering, University of Belgrade, Bulevar kralja Aleksandra 73, 11000 Belgrade, Serbia.

However, both methods required prior knowledge of the target's IR spectrum, an assumption that can be easily disqualified with today's counter-measure tactics. In [8] a new method based on the application of two sensors with the same spectral characteristics is proposed. This approach does not require a prior knowledge of the target's IR spectrum, providing that some other problems, such as synchronization of the sensor movement, track-to-track association and so on, are solved properly. The solution is based on target state estimation, using the extended Kalman filter (EKF) with the measurement vector augmented by the ratio of IR energy adsorbed by the sensors, simultaneously with recursive estimation of the atmospheric attenuation parameter. A limitation of the algorithm proposed in [8] appears when the distance between the sensors and the target is less than the value determined by the maximum output power of the sensors. If target is near to one sensor, it operates close to the saturated area and provides unreliable data. This paper suggests a hybrid approach to target tracking problem based on estimation from two described algorithms: triangulation method and triangulation extended with sensors' IR energy ratio. Instead of simple switching between the algorithms, two estimations are merged with confidence parameter, which is result of fuzzy reasoning process. Fuzzy controller is designed in accordance to the problem approach [9], and it estimates working conditions of both algorithms, enabling smooth interchange to method which generates lower mean estimation error. The results presented through simulations and experimental data show that the proposed solution can be implemented in combat systems to enable more efficient operation under real battlefield conditions.

Ranging System Based on Angle Measurements and Extended Kalman Filtering: Method A1

Figure 1 illustrates the geometry relations among the target and passive sensors. The distance between sensors S_1 and S_2 is the baseline length *d*, while angles $\lambda_1, \lambda_2, \varphi_1,$ and φ_2 are the appropriate azimuths, and elevations, respectively. If the origin of the tracking coordinate system is located at the position of sensor S_1, the position of the target is expressed as:

$$x = \frac{d}{\tan(\lambda_1) - \tan(\lambda_2)}; \quad y = \frac{d \cdot \tan(\lambda_1)}{\tan(\lambda_1) - \tan(\lambda_2)}; \quad z = \tan(\varphi_1) \cdot \sqrt{x^2 + y^2} \tag{1}$$

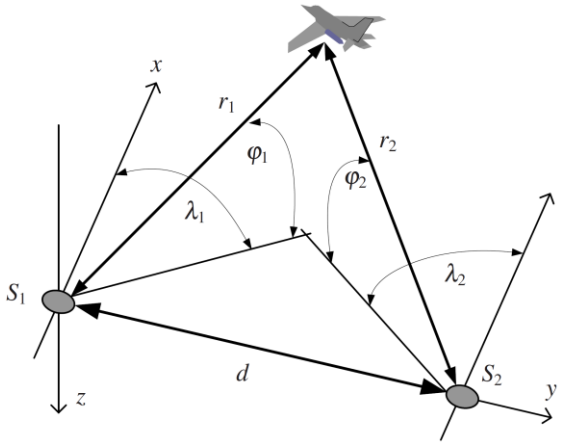

Fig. 1 Geometry Relations among the Target and Passive Sensors.

This method is frequently used in practice and is known as 'the principle of triangulation' [10]. Bearing in mind the stochastic nature of the target line of sight (LOS) angles, the EKF is used for target state estimation [10]. The target dynamics at the k^{th} sampling interval are modeled in the state space form as:

$$\mathbf{X}_1(k) = \mathbf{F}\mathbf{X}_1(k-1) + \upsilon(k-1) \tag{2}$$

In the above equation, $\mathbf{X_1}$ is the target state vector defined by:

$$\mathbf{X}_1 = \begin{bmatrix} x & \dot{x} & \ddot{x} & y & \dot{y} & \ddot{y} & z & \dot{z} & \ddot{z} \end{bmatrix}^{\mathrm{T}} \tag{3}$$

Matrix **F** in (2) is defined, for the sampling interval T as:

$$\mathbf{F} = \begin{bmatrix} \mathbf{G} & \mathbf{O_3} & \mathbf{O_3} \\ \mathbf{O_3} & \mathbf{G} & \mathbf{O_3} \\ \mathbf{O_3} & \mathbf{O_3} & \mathbf{G} \end{bmatrix}, \quad \mathbf{G} = \begin{bmatrix} 1 & T & T^2/2 \\ 0 & 1 & T \\ 0 & 0 & 1 \end{bmatrix} \tag{4}$$

where $\mathbf{O_3}$ is the square three-dimensional zero matrix. The random sequence $v(k-1)$ is a zero-mean white Gaussian state (process) noise with a known covariance matrix:

$$\mathbf{E}\left[\upsilon(k)\upsilon(j)^T\right] = \mathbf{Q}\delta(k,j) \tag{5}$$

where

$$\mathbf{Q} = \begin{bmatrix} \mathbf{U} & \mathbf{O_3} & \mathbf{O_3} \\ \mathbf{O_3} & \mathbf{U} & \mathbf{O_3} \\ \mathbf{O_3} & \mathbf{O_3} & \mathbf{U} \end{bmatrix}, \quad \mathbf{U} = \begin{bmatrix} T^4/4 & T^3/3 & T^2/2 \\ T^3/3 & T^2 & T \\ T^2/2 & T & 1 \end{bmatrix} q \tag{6}$$

with q being the variance of the process or state noise, and $\delta(k, j)$ being the Kronecker delta symbol. Discrete time measurements are modeled as:

$$\mathbf{Z}_1(k) = h\left[\mathbf{X}_1(k)\right] + w(k), \quad k = 0,1,2,... \tag{7}$$

where $\mathbf{Z_1}(k)$ is the four-dimensional vector that consists of target azimuth and elevation angles $[\lambda_1, \varphi_1, \lambda_2, \varphi_2]^{\mathrm{T}}$. The non-linear function $h[\mathbf{X}_1(k)]$ stands for transformations from Cartesian to polar coordinates, which are given by:

$$\begin{aligned} \lambda_1 &= \tan^{-1}\left(\frac{y}{x}\right), & \varphi_1 &= \tan^{-1}\left(\frac{-z}{\sqrt{x^2+y^2}}\right), \\ \lambda_2 &= \tan^{-1}\left(\frac{y-d}{x}\right), & \varphi_2 &= \tan^{-1}\left(\frac{-z}{\sqrt{x^2+(y-d)^2}}\right), \end{aligned} \tag{8}$$

The random sequence $w(k)$ represents a zero-mean white Gaussian measurement noise with a known covariance matrix, that is:

$$\mathbf{E_1}\left[w(k)w(j)^T\right] = \mathbf{R_1}\delta(k,j), \quad \mathbf{R_1} = \mathrm{diag}\left[\sigma_\lambda^2\ \sigma_\varphi^2\ \sigma_\lambda^2\ \sigma_\varphi^2\right] \tag{9}$$

with $\sigma_\lambda^2, \sigma_\varphi^2$ being the variances of angle measurement noises. The EKF equations (in the usual notation) are [10, 11]:

$$\bar{\mathbf{P}}_1(k) = \mathbf{F}\hat{\mathbf{P}}_1(k-1)\mathbf{F}_1^{\mathrm{T}} + \mathbf{Q} \tag{10}$$

$$\mathbf{S}_1(k) = \mathbf{H_1}(k)\,\bar{\mathbf{P}}_1(k)\,\mathbf{H_1^T}(k) + \mathbf{R_1} \tag{11}$$

$$\mathbf{K}_1(k) = \bar{\mathbf{P}}_1(k)\,\mathbf{H_1^T}(k)\,\mathbf{S_1^{-1}}(k) \tag{12}$$

$$\hat{\mathbf{P}}_1(k) = \bar{\mathbf{P}}_1(k) - \mathbf{K_1}(k)\cdot\mathbf{H_1}(k)\bar{\mathbf{P}}_1(k) \tag{13}$$

where $\mathbf{H_1}(k)$ is Jacobian matrix:

$$\mathbf{H}_1 = \begin{bmatrix} \partial\lambda_1/\partial x & 0 & 0 & \partial\lambda_1/\partial y & 0 & 0 & 0 & 0 & 0 \\ \partial\varphi_1/\partial x & 0 & 0 & \partial\varphi_1/\partial y & 0 & 0 & \partial\varphi_1/\partial z & 0 & 0 \\ \partial\lambda_2/\partial x & 0 & 0 & \partial\lambda_2/\partial y & 0 & 0 & 0 & 0 & 0 \\ \partial\varphi_2/\partial x & 0 & 0 & \partial\varphi_2/\partial y & 0 & 0 & \partial\varphi_2/\partial z & 0 & 0 \end{bmatrix} \tag{14}$$

with elements expressed as a result of partial derivation of (8):

$$\begin{aligned} &\frac{\partial\lambda_1}{\partial x} = \frac{-y}{x^2+y^2}; \quad \frac{\partial\lambda_1}{\partial y} = -\frac{\partial\lambda_1}{\partial x}\frac{x}{y}; \quad \frac{\partial\varphi_1}{\partial x} = -\frac{zx\,(x^2+y^2)^{-1/2}}{x^2+y^2+z^2}; \quad \frac{\partial\varphi_1}{\partial y} = \frac{\partial\varphi_1}{\partial x}\frac{y}{x}; \\ &\frac{\partial\varphi_1}{\partial z} = -\frac{\partial\varphi_1 x^2}{\partial x}\frac{x^2+y^2}{zx}; \quad \frac{\partial\lambda_2}{\partial x} = \frac{-(y-d)}{x^2+y^2}; \quad \frac{\partial\lambda_2}{\partial y} = -\frac{\partial\lambda_2}{\partial x}\frac{x}{y-d}; \\ &\frac{\partial\varphi_2}{\partial x} = -\frac{zx\left(x^2+(y-d)^2\right)^{-1/2}}{x^2+(y-d)^2+z^2}; \quad \frac{\partial\varphi_2}{\partial y} = \frac{\partial\varphi_2}{\partial x}\frac{y-d}{x}; \\ &\frac{\partial\varphi_2}{\partial z} = -\frac{\partial\varphi_2 x^2}{\partial x}\frac{x^2+(y-d)^2}{zx} \end{aligned} \tag{15}$$

The appropriate elements are calculated by means of the state predictions $\hat{x}(k|k-1)$, $\hat{y}(k|k-1)$, $\hat{z}(k|k-1)$, instead of the unknown real values x, y, z, respectively. Using the last measurement $\mathbf{Z}_1(k)$ and its predicted value $\bar{\mathbf{Z}}_1(k)$, the state update equation is given by:

$$\hat{\mathbf{X}}_1(k) = \bar{\mathbf{X}}_1(k) + \mathbf{K}_1(k)\left[\mathbf{Z}_1(k) - \bar{\mathbf{Z}}_1(k)\right] \tag{16}$$

where $\bar{\mathbf{Z}}_1(k)$ is calculated according to (8), together with the corresponding elements of the state prediction vector:

$$\bar{\mathbf{X}}_1(k) = \mathbf{F}\,\hat{\mathbf{X}}_1(k-1) \tag{17}$$

Target movement is tracked by an appropriate servo system, which minimizes the displacement of LOS relative to the pointing direction of the sensor.

Ranging System Based on Augmented Measurement Vector and Extended Kalman Filtering: Method A2

GDOP problem can be overcome extending the measurement vector by the appropriate intensity measurements of the target IR radiation. The irradiance W, at some distance r from the source emitting radiation through a gaseous atmosphere, may be calculated according to:

$$W = \tau_a \frac{I}{r^2} \tag{18}$$

where I is intensity of radiation emitted by source, and τ_a is the atmospheric transmittance over a designated path ($\tau_a \leq 1$). Atmospheric transmittance τ_a is a function of wavelength, path length, pressure, temperature, humidity and the composition of the atmosphere. The factor τ_a defines the decrease in radiant intensity because of absorption and scattering losses along the atmospheric path [12].

Assuming narrow wavelength bands and transmission on a horizontal path through an atmosphere of uniform composition, the transmittance of the atmosphere τ_a over a path length r for radiation of wavelength λ may be expressed by:

$$\tau_a = \exp(-\sigma_a r) \tag{19}$$

where σ_a is the spectral attenuation. Accordingly, based on the geometry shown in Fig. 1, the irradiances W_1 and W_2 that are measured at positions S_1 and S_2 can be expressed as:

$$W_i = \frac{I}{r_i^2}\exp(-\sigma_a r_i) + C\,\xi_i; \qquad i = 1,2 \tag{20}$$

The second term in (20) represents background noise irradiance, where C is an unknown parameter that describes the intensity of this noise, and ξ_i , $i = 1,2$ is the random variable with a Rayleigh distribution and a unity mean value [12]. The ratio of the irradiances W_1, W_2 that are measured at positions S_1 and S_2 can be expressed as:

$$\frac{W_2}{W_1} = \frac{\left(I/r_2^2\right)\exp\left(-\sigma_a r_2\right) + C\,\xi_2}{\left(I/r_1^2\right)\exp\left(-\sigma_a r_1\right) + C\,\xi_1} \tag{21}$$

In the ideal case, in the absence of background noise irradiance ($\xi_1 = \xi_2 = 0$), the theoretical value of this ratio would be:

$$\frac{W_2}{W_1} = \frac{r_1^2}{r_2^2}\exp\left(-\sigma_a\left(r_2 - r_1\right)\right) \tag{22}$$

However, the presence of background noise irradiance creates a shift from this theoretical value, and this shift can be modeled as a random variable ξ_3.

$$\frac{W_2}{W_1} = \left(\frac{W_2}{W_1}\right)_r + \xi_3 = w = \frac{r_1^2}{r_2^2}\exp\left(-\sigma_a\left(r_2 - r_1\right)\right) + \xi_3 \tag{23}$$

Based on (21) and (23) this random variable ξ_3 may be expressed as a function of variables ξ_1, ξ_2 and ranges r_1 and r_2:

$$\xi_3 = \frac{\left(I/r_2^2\right)\exp\left(-\sigma_a r_2\right) + C\,\xi_2}{\left(I/r_1^2\right)\exp\left(-\sigma_a r_1\right) + C\,\xi_1} - \frac{r_2^2}{r_1^2}\exp\left(-\sigma_a\left(r_2 - r_1\right)\right) \tag{24}$$

It is reasonable to use the measurable ratio w as an additional input for EKF, while ξ_3 may be considered an additive measurement noise. Beginning with the assumption that the random variables ξ_1 and ξ_2 are independent, analysis presented in [8] points out that the mean value of ξ_3 is negligible if the background noise irradiance C is low enough, compared to the irradiances W_1 and W_2. In this case, the EKF with an extended measurement vector $\mathbf{Z}_2(k)$ consisting the appropriate angles (the target azimuth and elevations relative to both sensors), and the ratio of irradiances $W_2/W_1 = w$ is employed; that is:

$$\mathbf{Z}_2 = \begin{bmatrix}\lambda_1 & \varphi_1 & \lambda_2 & \varphi_2 & w\end{bmatrix}^{\mathrm{T}} \tag{25}$$

The measurement matrix $\mathbf{H_1}$ must also be augmented with the additional row:

$$\mathbf{H}_w = \begin{bmatrix}\partial w/\partial x & 0 & 0 & \partial w/\partial y & 0 & 0 & \partial w/\partial z & 0 & 0\end{bmatrix} \tag{26}$$

where:

$$w = \frac{W_2}{W_1} \approx \frac{r_1^2}{r_2^2}\exp\left(-\sigma_a\left(r_2 - r_1\right)\right) \tag{27}$$

and the appropriate elements are given by:

$$\frac{\partial w}{\partial x}=\frac{r_1^2}{r_2^2}e^{\sigma_a(r_2-r_1)}\left(\frac{2+\sigma_a r_1}{r_1^2}-\frac{2+\sigma_a r_2}{r_2^2}\right)x;$$
$$\frac{\partial w}{\partial y}=\frac{\partial w}{\partial x}\frac{y}{x}+\frac{r_1^2}{r_2^2}e^{\sigma_a(r_2-r_1)}\left(\frac{2+\sigma_a r_2}{r_2^2}\right)d; \qquad \frac{\partial w}{\partial z}=\frac{\partial w}{\partial z}\frac{z}{x} \tag{28}$$

Of course, the distances:

$$r_1=\sqrt{x^2+y^2+z^2} \qquad \text{and} \qquad r_2=\sqrt{x^2+(y-d)^2+z^2} \tag{29}$$

are calculated as before, based on the predictions of the target $\hat{x}(k|k-1)$, $\hat{y}(k|k-1), \hat{z}(k|k-1)$ instead of the real unknown values *x, y, z,* respectively. The approximation (27) is obtained by neglecting the second terms in the appropriate expression (23), since these terms are significantly smaller than the first terms which apply when an actual target is present. It is evident from the above that instead of the matrix $\mathbf{H_1}$ in (14), the new measurement matrix should be defined as:

$$\mathbf{H_2}=\left[\mathbf{H_1^T} \quad \mathbf{H_w^T}\right]^{\mathbf{T}} \tag{30}$$

and the corresponding covariance matrix $\mathbf{R_2}$:

$$\mathbf{R_2}=\mathrm{diag}\left[\mathrm{diag}(\mathbf{R_1}) \quad \sigma_w^2\right] \tag{31}$$

should be used instead of the matrix $\mathbf{R_1}$ in (9), with σ_w^2 being the variance of the irradiance ratio *w*. A detailed analysis of the statistical properties of the random variable ξ_3, which is presented in the [8], shows that for different target flight scenarios and sensor characteristics the variance of this random variable does not exceed 0.008 ($\sigma_w^2 \leq 0.008$). As such, in order to obtain a robust estimation of the signals, the maximum value σ_w^2 = 0.008 can be adopted in defining the covariance matrix $\mathbf{R_2}$.

Fuzzy Controller Design

Analysis in [8] shows that methods for passive target tracking, named A1 and A2, have various advantages, but some disadvantages in special configurations still remain. The method A2 is superior in cases when the target is distanced from both sensors; hence method A1 generates more acceptable results in cases when one of the sensors operates close to the saturation, and if the geometric dilution of precision is not apparent. The main goal of this research is to join estimations from methods A1 and A2 in one single hybrid estimation. The state vector estimations of the methods A1 and A2 is denoted by $\hat{\mathbf{X}}_1(k)$ and $\hat{\mathbf{X}}_2(k)$ respectively, and the final state estimation is computing from the following equation:

$$\hat{\mathbf{X}}_H(k)=\hat{\mathbf{X}}_1(k)\cdot(1-\zeta(k))+\hat{\mathbf{X}}_2(k)\cdot\zeta(k) \tag{32}$$

where $\zeta(k)$ is the nonnegative scalar, and can assume values from the interval [0,1]. If one of the sensors operates close to saturation, then parameter ζ is close to zero, whereas for the large dilution of precision and large values of r_1 and r_2, parameter ζ is close to one. This linguistic interpretation of solution for the problem of synergy of two target tracking algorithms is convenient for translation into the language of if-then rules, and it is well known that fuzzy logic is most effective when point of departure is a human solution [13].

For the subject case, the selected output variable of the FLC is the parameter ζ, and the interval [0,1] is selected as the domain of membership functions attributed to the output variable. The input variables of the FLC are the dilution of precision fuzzified measure- f_{DOP}

and distances relative to sensors. Figure 2 shows the membership functions of the linguistic variables distances r_i, i = 1,2. Variables r_1, and r_2 signify the distances between the target and the first and second sensors respectively.

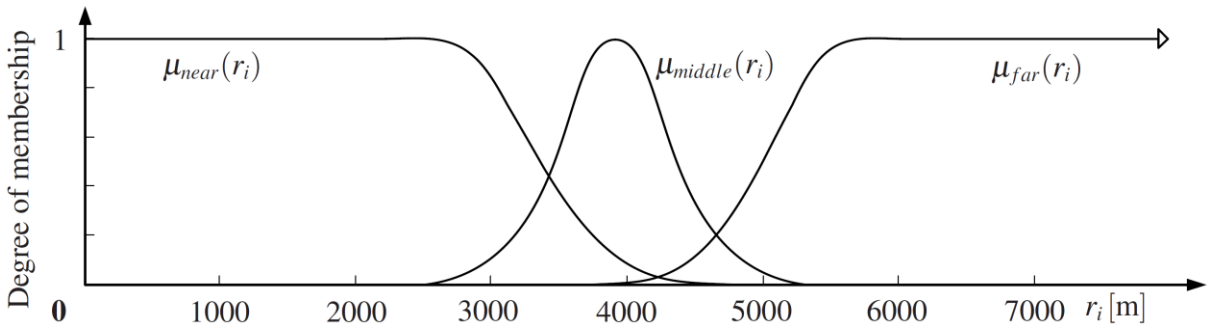

Fig. 2 Definition of Membership Functions for Distances r_i , i = 1,2

The linguistic variable $distance$ is defined through three membership functions: $near$, $middle$ and *far*, whose parameters are adjusted in accordance with results presented in [8]. Accuracy decreasing of the triangulation method A1 is detectable in case where angle λ_1 is approximately equal to the angle λ_2, what is potential outcome of two scenarios. For large distances r_1 and r_2, angle λ_1 is close to λ_2, in which case algorithm A2 generates better estimation [8]. In the second scenario, when the target directions λ_1 and λ_2, are nearly collinear relative to the baseline, method A1 produces unacceptable results [8]. The third input of hybrid fuzzy target tracking algorithm is linguistic variable fuzzy dilution of precision - f_{DOP}, which denotes the fuzzy measure of collinearity of the directions to the target, formed based on:

$$f_{DOP} = |\lambda_1 - \lambda_2| \tag{33}$$

and the corresponding membership functions are shown in Fig. 3.

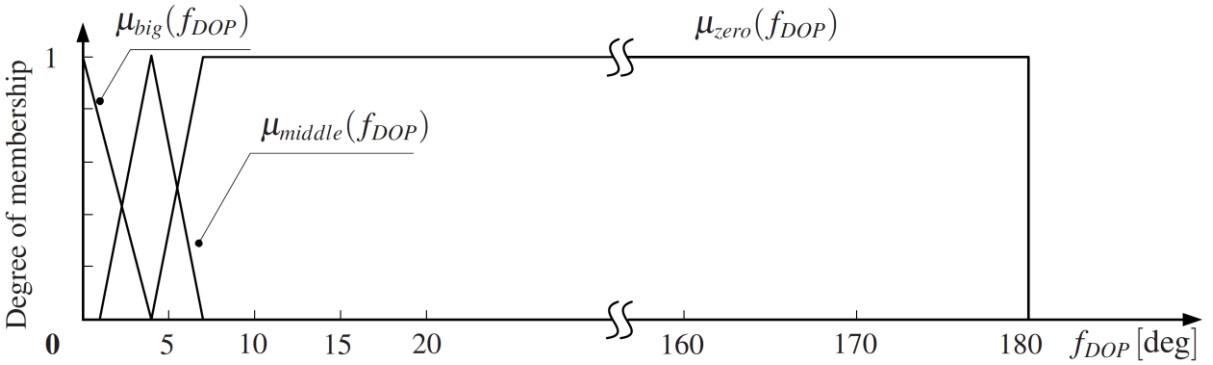

Fig. 3 Definition of Membership Functions for Linguistic Variable f_{DOP}

Membership function big denotes the major dilution of precision, and the results of the algorithm A1 are almost unacceptable. In the case when values of f_{DOP} are fitted in membership function $middle$, results of algorithm A1 can be accepted with more confidence, especially if algorithm A2 operates in poor defined area (short distances to sensors). If f_{DOP} is zero and distances to sensors are short, then the outputs of algorithm A1 should be taken as the outputs of hybrid algorithm. The designed FLC is of the Takagi-Sugeno type, with three inputs: two distances between the target and the sensors (r_1 and r_2) and the fuzzy dilution of precision - f_{DOP}, and one output: confidence parameter ζ. For **T**-norm, the minimum method was selected, and for **S** norm the maximum method was selected. The fuzzy rules base for hybrid target tracking algorithm are shown in Table 1.

The set of rules is comprised of 27 rules, and rules are defined in accordance with preceding considerations. Namely, when estimated distance to the target is big, relative to both sensors, maximal value is selected for parameter ζ, and advantage is given to the A2 algorithm. Further, as these distances come shorter, the influence of A1 algorithm is increasing, according to the value of f_{DOP} variable. Figure 4 shows control surface for distances r_1 and r_2. Value of parameter f_{DOP} is fixed on 5 degrees. The control surface has two plateaus, one for $\zeta \approx 0$, when the distances r_1 and r_2 are short, and other for $\zeta \approx 1$, when r_1 and r_2 have large values. Tuning of hybrid fuzzy regulator is done via computer simulations for different initial conditions and target's trajectories.

Table 1. Hybrid Algorithm - Fuzzy Rules Base.

Rule	r_1	r_2	f_{DOP}	ζ
1.	*near*	*far*	*big*	1
2.	*near*	*far*	*middle*	1
3.	*near*	*far*	*zero*	1
4.	*near*	*middle*	*big*	0.5
5.	*near*	*middle*	*middle*	0.2
6.	*near*	*middle*	*zero*	0
7.	*near*	*near*	*big*	0.5
8.	*near*	*near*	*middle*	0
9.	*near*	*near*	*zero*	0
10.	*middle*	*far*	*big*	1
11.	*middle*	*far*	*middle*	1
12.	*middle*	*far*	*middle*	1
13.	*middle*	*middle*	*big*	1
14.	*middle*	*middle*	*zero*	0.5
15.	*middle*	*middle*	*zero*	0
16.	*middle*	*near*	*big*	0.5
17.	*middle*	*near*	*middle*	0.2
18.	*middle*	*near*	*zero*	0
19.	*far*	*far*	*big*	1
20.	*far*	*far*	*middle*	1
21.	*far*	*far*	*zero*	1
22.	*far*	*middle*	*big*	1
23.	*far*	*middle*	*middle*	1
24.	*far*	*middle*	*zero*	1
25.	*far*	*near*	*big*	1
26.	*far*	*near*	*middle*	1
27.	*far*	*near*	*zero*	1

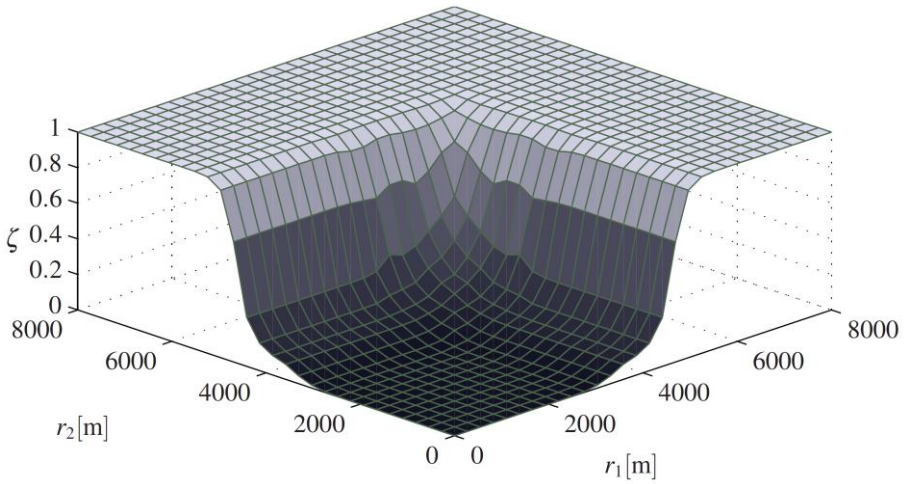

Fig. 4 Control Surface for Distances and f_{DOP} = 5°00′00″.

Hybrid Algorithm Description

We propose a new hybrid structure, shown in Fig. 5. System's input variables are the azimuth and elevations relative to both sensors $[\lambda_1, \varphi_1, \lambda_2, \varphi_2]^T$, and the ratio of irradiances W_2/W_1. Algorithm 1 utilizes azimuths and elevations, and Algorithm 2 takes into account all input variables. Extinction coefficient σ_a (block **f**) is estimated according to [14]. Algorithms 1 and 2, and fuzzy logic controller (FLC) work in parallel. Final state estimations are produced in block (**g**).

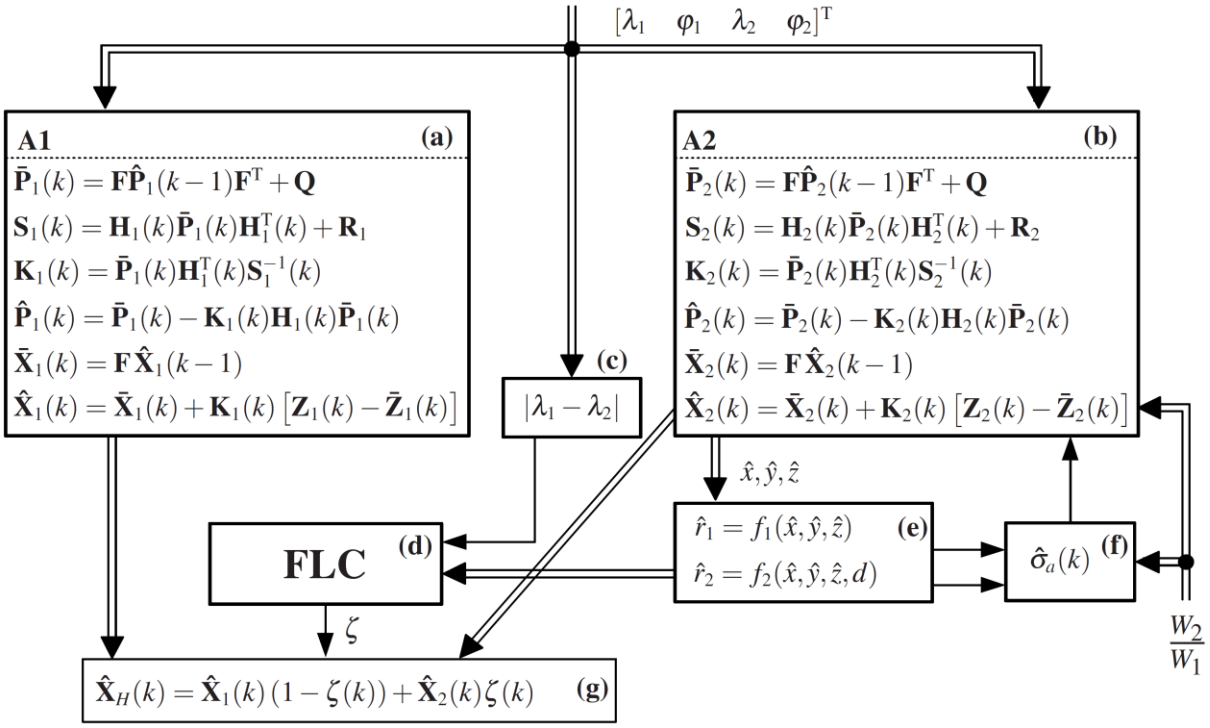

Fig. 5 Hybrid Algorithm Block Diagram

Simulation Results

The scenario based on which the flight of the target was simulated is as follows: the initial position of the target was determined by the vector [x(0),y(0),z(0)] = [5000,300, —600], with the initial velocity vector [$v_x(0)$, $v_y(0)$, $v_z(0)$] = [-7, -5, -1]. During the simulation there were accelerations along x-, y-, and z-axes, a_x = 6, a_y = -3, and a_z = -1. All quantities are given in SI metric system. The kinematics initial conditions of the target were assumed to be:

$$\hat{x}(0) = 4950\text{m} \qquad \hat{y}(0) = 320\text{m} \qquad \hat{z}(0) = -620\text{m} \tag{34}$$

Other initial conditions were assumed to be zero. The sampling time of the measurements was T = 1s and the adopted baseline length was d = 2km. The target trajectory (its yx projection) is presented in Fig. 6a, whereas the corresponding azimuth measurements are shown in Fig. 6b. The sensors are located in positions (x = 0, y = 0, z = 0) and (x = 0, y = d , z = 0).

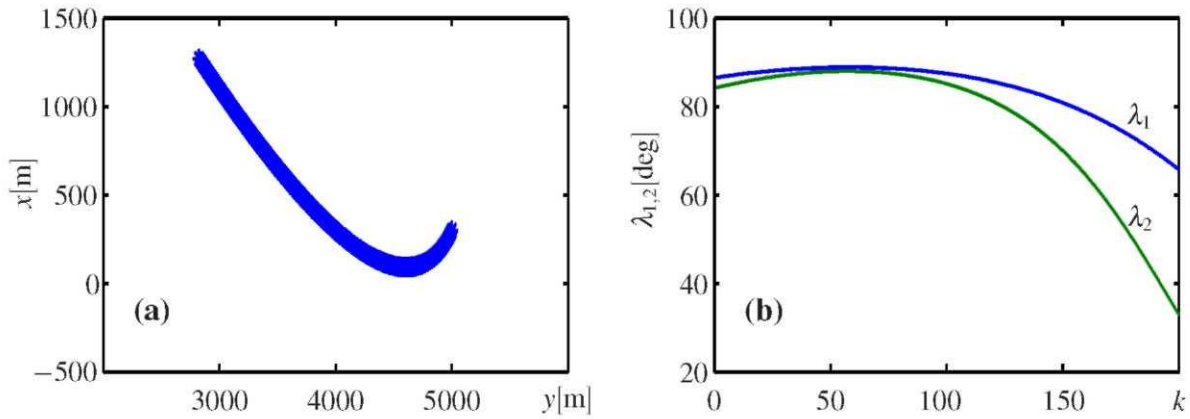

Fig. 6 (a) The yx Projection of the Target Trajectory; (b) Measured Azimuths Angles

The first part of the trajectory represents a case where the target LOS and the baseline are almost collinear. This situation is recognizable since the azimuth angles are very close to each other, and are both close to 90 degrees, during this part of the trajectory. The appropriate matrices for extended Kalman filters shown in Fig. 5 are adopted according to [8]. Figure 7 illustrates the absolute error of distance estimation generated by algorithms A1, A2 and FLC.

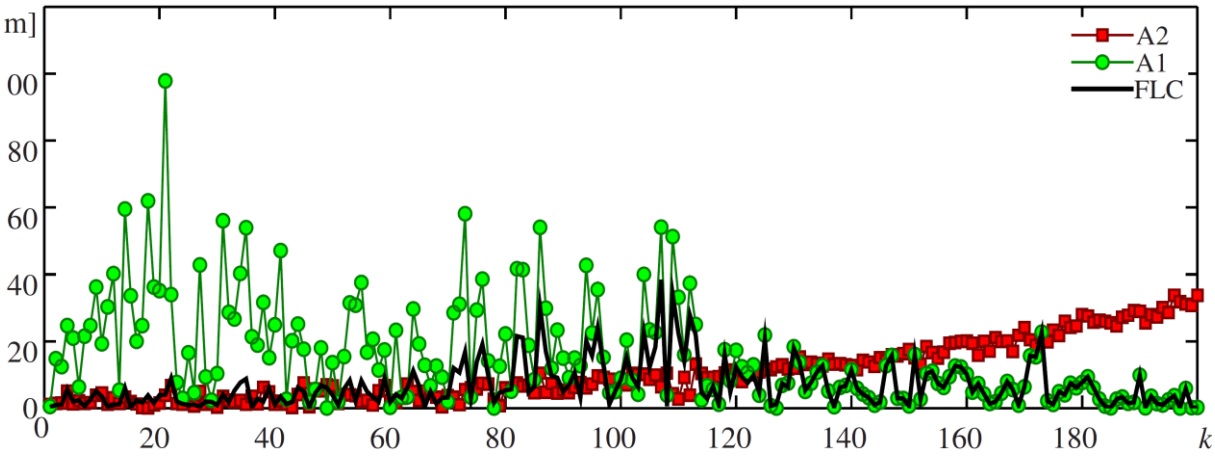

Fig. 7 Absolute Error of Distance Estimation by Algorithms A1, A2 and FLC

Comparison between algorithms A1 and A2 (Fig. 7) during the first half of the trajectory shows that algorithm A2 was superior, since the information in the irradiances W_1 and W_2, although corrupted by considerable measurement noise, was useful and allowed for estimation quality improvement. On the other hand, during the second half of the trajectory, the saturation effect that appeared in the irradiance measurement W_2 became significant and, consequently, the adopted relation between this irradiance and the distance (20) was no longer valid. In such cases, the extended input W_2/W_1 becomes useless and, furthermore, destructive, resulting in a performance degradation of algorithm A2.

The designed hybrid algorithm based on FLC merges outputs of algorithms A1 and A2 in an expected way, as shown in Fig. 7. At the beginning of the simulation parameter ζ (32) is close to one (Fig. 8), and output of hybrid controller is close to the outputs estimated by algorithm A2. During the second half of the trajectory parameter ζ is closing to zero and outputs of the hybrid system are therefore close to the states estimated by algorithm A1. In the middle of the simulation algorithms A1 and A2 were generated more or less comparable outputs, and the error in distance estimation produced by hybrid algorithm in this part of the simulation is among A1 and A2 errors.

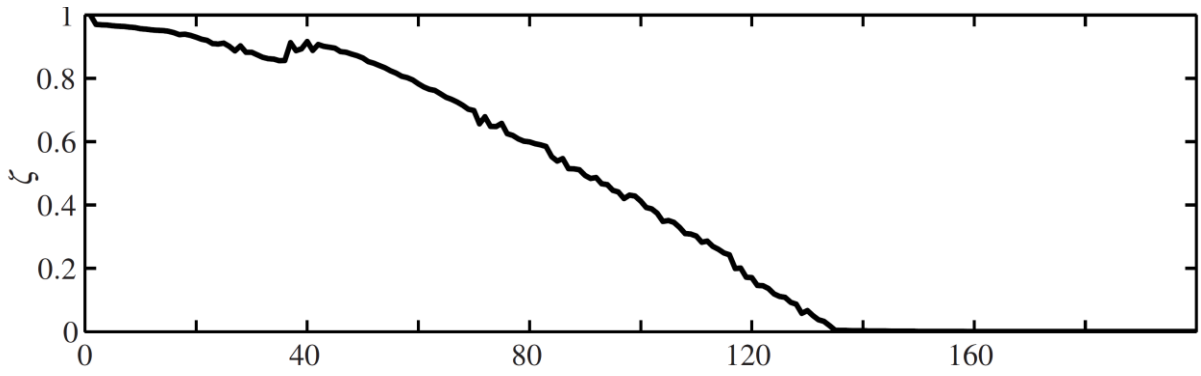

Fig. 8 FLC Output, the Parameter ζ

Experimental Results

In order to demonstrate the applicability of the proposed hybrid approach, real data studied in [8] were reanalyzed. Two passive (IC) sensors, located at a distance of d = 2km, were recording the irradiance of a low altitude airplane. The altitude was almost constant (50m), and the duration of recording was 16s with a sampling ratio of six samples/s (93 samples were made available). The azimuth and elevation angles of the servo-mechanisms carrying the sensors are shown in Fig. 9.

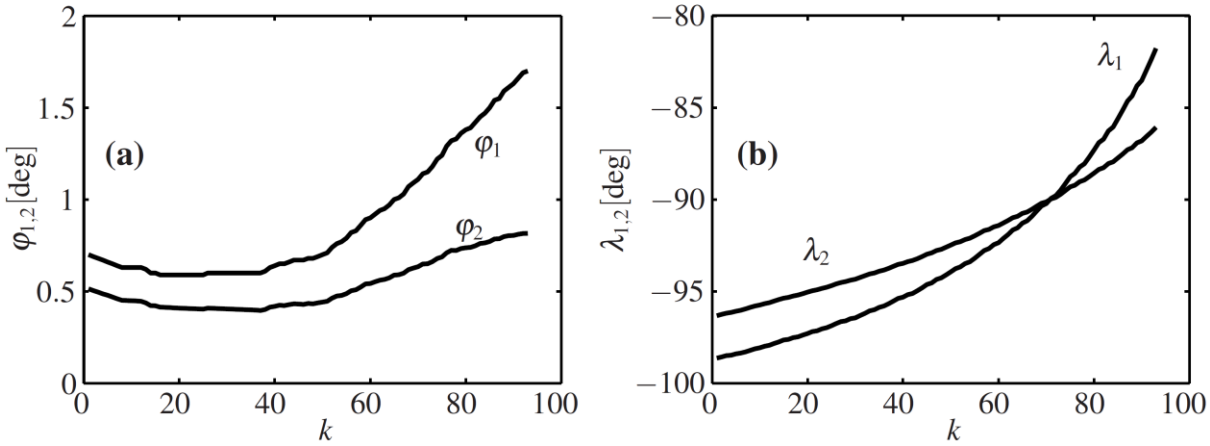

Fig. 9 (a) Measurement Sequences: Elevation Angles; (b) Azimuth Angles

The irradiances were obtained directly by measuring the sensors' output voltage, with no additional filtering. The adopted covariance matrices for the EKF were the same as in the previous simulation example. In order to compare the results, we used the available measured distance between the airplane and the first sensor. This distance was measured by a high-precision radar and it is shown in Fig 10a. Figure 10b presents the absolute error between the measured and estimated distance generated by algorithms A1, A2 and hybrid algorithm (FLC).

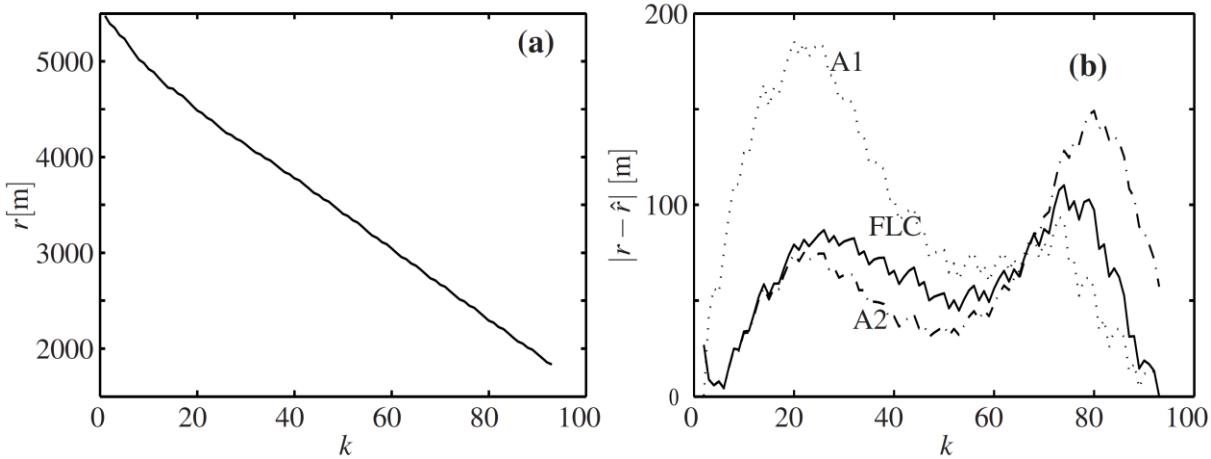

Fig. 10 Experimental Results: (a) True Distance between the Target and the First Sensor Measured by Radar; (b) Absolute Error of Distance Estimation Generated by Algorithms A1, A2 and FLC.

There is no superior algorithm during the whole experiment. During the first half of the trajectory the algorithm A2 produced the smallest estimation error, while during the second half of the experiment algorithm A1 was superior. Hybrid approach merges these results in an expected way, like in previous simulation experiment, and therefore generates the most acceptable results during the entire experiment.

Conclusion

This paper considers the problem of target tracking with two passive IR non-imaging sensors. Beginning with the EKF solution based on the triangulation principle, and the algorithm using the extension of the measurement vector with the ratio of IR energy adsorbed by sensors, a new hybrid approach to passive ranging is proposed. Hybrid algorithm, which is based on fuzzy reasoning, is examining target tracking conditions, and estimating confidence of both algorithms. Based on estimated confidence parameter, results from two algorithms are merged in an ultimate solution, which has lower mean error over tracking interval than input algorithms autonomously.

The results obtained through simulations and experimental data show that the proposed solution can be implemented in combat systems to enable more efficient operation under real battlefield conditions. The accuracy in the case of single-baseline passive ranging systems can be significantly improved by the application of the proposed hybrid solution in situations where the target is close relative to the tracking sensors.

References

[1] Dufour F. and Mariton. M. "Tracking a 3D Maneuvering Target with Passive Sensors", IEEE T Aero Elec Sys, 1991, Vol. 27, pp. 725-739.

[2] Masayoshi I., Tsujimichi S. and Kosuge Y. "Tracking a Three-dimensional Moving Target with Distributed Passive Sensors Using Extended Kalman Filter", Electron Commun JPN, 2001, Vol. 84, pp. 74-85.

[3] Jinsheng L., Zuoliang L. and Honggang D. "Heterogeneous Sensors Data Fusion for Target Tracking", *Signal Processing Proc., 4th Int. Conf.,* 1998, Vol. 2, pp. 1525-1528.

[4] De Visser M., Schwering P., De Groot J. and Hendriks E. "Passive Ranging Using an Infrared Search and Track Sensor", Opt Eng, 2006, Vol. 45, p. 026402.

[5] Pieper J.R., Coper A.W. and Pelegris G. "Passive Range Estimation Using Dual-baseline Triangulation", Opt Eng, 1996, Vol.35, pp. 685-692.

[6] Ovrebo J.P. and Wood R.C. "Apparatus for Passive Infrared Range Finding", 1963. US Patent 3,103,586.

[7] Jennes J.R. and Shimukonis F.J. "Apparatus for Passive Infrared Range Finding", 1964, US Patent 3,117,228.

[8] Durovic Z.M, Kovacevic B.D., and Dikic G.D. "Target Tracking with Two Passive Infrared Non-imaging Sensors", IET Signal Process, 2009, Vol. 3, pp. 177-188.

[9] Mitrovic S.T. and Durovic Z.M., "Fuzzy Logic Controller for Bidirectional Garaging of a Differential Drive Mobile Robot", Adv Robotics, 2010, Vol. 24, pp. 1291-1311.

[10] Bar-Shalom Y. and Li. X.R. "Multitarget-Multisensor Tracking: Principles and Techniques", Clearance Center, Danvers, MA, 1995.

[11] Kovacevic B. and Durovic Z.M., "Fundamentals of Stochastic Signals, Systems and Estimation Theory with Worked Examples", Springer Verlag, 2008.

[12] Drigers R.G., Cox P. and Edwards T., "Introduction to Optoelectronic Systems". Artech House, New York, 1999.

[13] Zadeh. L.A. Outline of a Computational Theory of Perceptions Based on Computing with Words. In N.K. Sinha, M.M. Gupta, and L.A. Zadeh, editors, *Soft Computing and Intelligent Systems: Theory and Applications,* pp 2-22. Academic Press, 2000.

[14] Dikic G.D. and Durovic Z.M., "Unbiased Estimation of Atmosphere Attenuation Coefficient", Electr Eng, 2007, Vol. 89 pp. 343-347.